

# Photocatalytic Analysis on WO<sub>3</sub> Nanoparticles

V. Hariharan<sup>2\*</sup>, V. Aroulmoji<sup>2</sup>, M. Mala<sup>1</sup>, V. Karthik<sup>1</sup>

<sup>1</sup>PG & Research Department of Physics, Mahendra Arts and Science College (Autonomous), Kalipatti, Namakkal District – 637 501, Tamilnadu, India

<sup>2</sup>Center for Research and Development, Mahendra Engineering College (Autonomous), Mallasamudram, Namakkal District - 637 503, Tamilnadu, India

**ABSTRACT:** Pure and doped WO<sub>3-x</sub> nanoparticles were prepared by facile microwave irradiation method and investigated for strong photocatalytic activity due to the great importance of oxygen vacancies (V<sub>O</sub>). In the present study, pure and "Fe (~3wt.%) " doped WO<sub>3-x</sub> nanoparticles and their crystalline nature were evaluated using powder X-ray diffraction (XRD). Bandgap analysis on W17047 has band gap values due to the movement of oxygen vacancies. The morphological nature of the prepared products was observed by FE-SEM analysis. The observed photocatalytic behavior of the prepared compounds under visible light irradiation and the corresponding efficiency was found to be more than 50%.

**KEYWORDS:** Tungsten oxide, microwave irradiation, photocatalytic, iron doped metal oxide, semiconducting metal oxides.

<https://doi.org/10.29294/IJASE.8.4.2022.2467-2476> ©2022 Mahendrapublications.com, All rights reserved

## 1. INTRODUCTION

In recent centuries, nano semiconducting metal-oxides nanomaterials have created more attention due to their advanced physio chemical properties along with biological properties in different areas of research that includes biotechnology, biomedical and medicine. On the other hand, Infections due to bacteria's are nowadays considered as an important threat to the human populations. In focus, the various ideas and approaches in order to deal this antibacterial activity, especially nanoscale semiconductor based metal oxides, in focus tungsten oxide (WO<sub>3</sub>) is regarded as one of the promising semiconducting metal oxides ( band energy varies from 2.4 - 2.8 eV) due to its contributions towards the applications of sensors, smart windows, electrochemical activities, superconductors, and so on [1]. In addition with the above recent literatures about tungsten oxide (WO<sub>3</sub>) show a remarkable functioning of this material in the field of antibacterial activity applications and their relevant biological applications. However, it is also to be considered that WO<sub>3</sub> alone is not having an remarkable antibacterial properties due to its various stoichiometric nature [2,3]. Hence, it has been reported that various dopants with transition metals such as Ag, Cu, Fe, Mn, etc., may enhance the antibacterial

activity due to the successful electron recombination process of WO<sub>3</sub> [4]. In literature point of views, Umair Baing et al., [5] synthesized silver decorated tungsten trioxide (WO<sub>3</sub>) semiconducting nanoparticles using facile wet impregnation technique for inactivation of harmful water-borne gram-negative pathogens. They found that morphogenesis by electron microscopy revealed the close contact of nanomaterials with the bacterial cell wall and membrane leading to severe damage to the integrity of membrane which caused cell death. Guangxin Duan et.al., [3] analyzed the robust antibacterial activity of WO<sub>3</sub> nanodots by simple one pot synthesis approach. Their findings suggested that oxygen deficient (WO<sub>3-x</sub>) nanodots have considerable potential impact in antibacterial applications, while also being biocompatible at large.

Rupy Kaur Matharu [6] dealt various antimicrobial strategies, that include antibiotics with some surface modifications to medical facilities and instruments and that has been devised in an attempt to reduce the incidence of nosocomial infections. They studied and suggested that tungsten oxide/polymer nanocomposite promotes the mediation of inhibition of microbial growth in suspension.

\*Corresponding Author: vhariharan06@yahoo.com

Received: 10.04.2022

Accepted: 20.05.2022

Published on: 18.05.2022

Hariharan et al.,

Jeevitha et al., [7] made an attempt to create a platform with the help of Tungsten oxide-graphene oxide (WO<sub>3</sub>-GO) nanocomposite. The nanocomposite is useful for various applications like degrades methylene blue and indigo carmine dyes, enhanced antibacterial activity and also useful for antibacterial and anticancer agent. Han et al., [8] used facile ultrasonic assisted technique in the syntheses of orthorhombic WO<sub>3</sub> nanoparticles. The cytotoxicity of dextran-stabilized and nonstabilized WO<sub>3</sub> sols was studied in vitro using dental pulp stem (DPS) cell lines and breast cancer (MCF-7) cell lines. Tungsten oxide sols demonstrated low cytotoxicity and low genotoxicity for both stem cells and malignant cells. Maqsood Ahamad et al., [9] studied antimicrobial properties of copper oxide nanoparticles (CuO) synthesized using facile precipitation technique. It showed effective antimicrobial activities against *Escherichia coli*, *Pseudomonas aeruginosa*, *Klebsiella pneumonia*, *Enterococcus faecalis*, *Shigella flexneri*, *Salmonellatyphimurium*, *Proteus vulgaris*, and *Staphylococcus aureus*. On the other hand, Fariba Ghasempour et al., [10] investigated Antibacterial activity of tungsten oxide nanorods/microrods were studied against *Escherichia coli* bacteria under visible light irradiation and in dark. They concluded that the nanorods of WO<sub>3</sub> showed a strong antibacterial property under visible light irradiation in addition with 92% bacterial inactivation within 24h irradiation at room temperature, while the K<sub>2</sub>W<sub>6</sub>O<sub>19</sub> microrods formed at 800°C could inactivate only approximately 45% of the bacteria at the same conditions. Baniker et al., [11] reported that linear models was used to investigate the effectiveness of three different metallic nanoparticles, tungsten carbide (WC), silver (Ag) and copper (Cu), in combination and separately. Results showed that when the nanoparticles are placed in combination (NPCs), antimicrobial effects significantly increase than when compared with SENPs (P < 0.01). Syed et al., [12] believed that the fabrication of tungsten (W) based nanoparticles on catheters could possibly prevent them from being contaminated by pathogens and hence provide continuous protection of the site. Raid A. Ismail et al., [13] utilized iron oxide nanoparticles by LASER ablation in liquid. They observed that the preparation conditions may affect the antibacterial activity of these prepared nanoparticles. The prepared iron oxide nanoparticles were used to capture rapidly S.

*aureus* bacteria under the magnetic field effect. Hasan Turkez et al., [14] investigated the toxicity potentials of WO<sub>3</sub> nanoparticles at various concentrations in cultured primary rat hepatocytes. These tests revealed that these nano particles did not cause any major significant increases of micronucleated hepatocytes (MNHEPs) but it showed the increase in 8-oxo-2-deoxyguanosine (8-OH-dG) levels when compare to that of control culture. Popov et al., [15] used WO<sub>3</sub> nano particles to induce hemolytic activity. It is attributed to the direct interaction of the nanoparticles with the RBCs, resulting in the oxidative stress, membrane injury, and subsequent hemolysis. Akbaba et al., [16] observed alterations in the micronucleus (MN) and the comet assay parameters revealed that WO<sub>3</sub> nanoparticles have genotoxic potential and could pose environmental and human health risk.

By bearing in mind the contributions of WO<sub>3</sub> nanodimensional materials in various fields, in the best of our knowledge through various literature, for the first time, this work will be a report on pure and "Fe" doped WO<sub>3</sub> nanodimensional materials in order to degrade Rhodamine B (RhB) for photocatalytic applications. Moreover, we report facile route to synthesis the proposed nanodimensional materials using cost effective and environmental friendly microwave irradiation technique. Also, the present work elaborates the synthesized nano materials have been characterized to know the structural, optical and microscopic nature of the materials to find out the suitability of the material for photocatalytic applications. Above all, this work demonstrates a pure and doped novel material for proposed photocatalytic applications for the first time.

## 2. MATERIALS AND METHODS

In the below procedure, Pure and "Fe" (~3wt.%) doped tungsten oxide (WO<sub>3</sub>) nano dimensional powders were prepared by using facile microwave irradiation method under ambient condition [17]. The elaborated experimental procedure is as follows: Analytical grade of 4.98g of tungstic acid (H<sub>2</sub>WO<sub>4</sub>) was dissolved in 20 mL of sodium hydroxide (NaOH) with one molar ratio. The yellow colored solution was stirred for 20 min in order to get uniform saturated solution. This resultant yellow colored hydrated sodium tungstate (Na<sub>2</sub>WO<sub>4</sub>.2H<sub>2</sub>O) solution was obtained due to

proton exchange protocol process [18] which has been given by the equation below. On the other hand, 3 wt.% of Ferrous sulfate ( $\text{Fe}_2\text{SO}_4 \cdot 7\text{H}_2\text{O}$ ) solution was prepared using deionized water and that was mixed along with sodium tungstate solution was stirred for 30 min. Both the solution was mixed slowly together and the final solution was stirred again for 30 min. The pH of the solution was neutral ( $\approx 7.0$ ) and it was tuned up to 1 by adding few drops of HCl because it may act as a precipitating agent and also suitable medium for the end products to have specific morphology [19]. In addition with that above solution 5 ml of double distilled water ( $\sim 50\%$  of precursor solution) was added in order to respond microwave quickly during irradiation process. In the progression, the final solution was transformed into a house hold microwave oven (2.45GHz and optimum power of 900W) since, microwaves allows the products with controlled shape and size.

Moreover, it minimizes the thermal gradients during synthesis process by manipulating nucleation growth and kinetics. In addition with the above, due to the difference in microwave extinction coefficient between the solvent and reactant along with the values of dielectric constants and selective dielectric heating rate can provide significant enhancement in the rate of chemical reaction. By bearing in mind the importance of microwave irradiation (MWI) over conventional heating methods, the conditions in microwave oven were set into 240 W for 10 min at room temperature for the synthesis of nano dimensional particles. A yellow colored precipitate was obtained after microwave irradiation process. The resultant powders were annealed in a muffle furnace at  $550^\circ\text{C}$  for 6 h in ambient conditions in order to remove the byproducts and to improve the crystallinity.

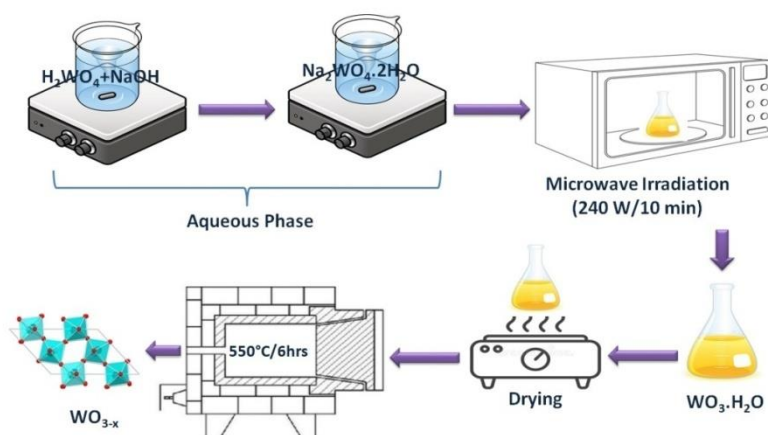


Fig.1: Schematic representation of the preparation by microwave irradiation method

### 3 RESULTS AND DISCUSSION

#### 3.1 Powder XRD analysis

Powder X-ray diffraction was carried out in order to know the crystalline nature of the resultant products within in the  $2\theta$  region from their respective bragg's angle is displayed in Fig. [2(a-d)]. It is clearly observed that all the diffraction patterns obtained from the diffraction pattern are in agreement with the reference JCPDS data indicating that the as prepared samples in the case of both pure and annealed samples could be assigned to a single orthorhombic phase [JCPDS card no: 43-0679] with high crystalline nature (Fig. 2a & 2c). Moreover, there is no evidence for secondary phase observed in the diffraction patterns implies that the dopant ion totally diffused into

$\text{WO}_3 \cdot \text{H}_2\text{O}$  and  $\text{WO}_{3-x}$  crystal lattice. In the case of pure and doped samples ( $\text{WO}_3 \cdot \text{H}_2\text{O}$ ) a small shift is observed in Bragg angle due to introduction of "Fe" ion in  $\text{WO}_3 \cdot \text{H}_2\text{O}$  crystal structure and it may due to the fact that "Fe" is having less atomic radius of around 126 pm when compared to that of tungsten ion (210 pm). It is to be noted that after doping it retains its original orthorhombic parent phase may be attributed to i) the replacement of "W" ion by "Fe" ion because of its substantial atomic radius ii) the low level of "Fe" for the formation of secondary phase. Also, it is observed that the variation in intensity of diffraction peaks in the case of pure and doped as prepared samples

implies that the variation in growth rate due to the incorporation of "Fe" ion. The crystallite for the resultant products was found to be 31.5, 11, 32.2 and 40 nm for the samples  $\text{WO}_3 \cdot \text{H}_2\text{O}$  &  $\text{WO}_3 \cdot \text{H}_2\text{O}$  (3wt.% Fe),  $\text{WO}_{3-x}$  and  $\text{WO}_3$  (3wt.% Fe) respectively using Debye Sherrer formula [20]. In the next step, Fig [2b & 2d] shows the XRD pattern of the annealed samples  $\text{WO}_{3-x}$  &  $\text{WO}_3$  (3wt.% Fe) respectively. The analysis confirms that the dopant free sample belongs to monoclinic phase ( $\text{W}_{17}\text{O}_{47}$ ) which is having the space group of  $P_{2/c}$  (JCPDS no.: 79-0171).

Interestingly, the doped samples show the stoichiometric  $\text{WO}_3$  with the monoclinic phase formation also in agreement with the reference (JCPDS no.: 83-0950). It is therefore understand that  $\text{Fe}^{2+}$  plays a dominant role in fixing the oxygen content of the end products. The crystallite size shows the increase in size is due to the minimization of oxygen losses [21]. Moreover, electro statistically the oxygen vacancies reduces hole which gives rise to acceptors [22] which is in agreement with the Diffuse reflectance spectral analysis.

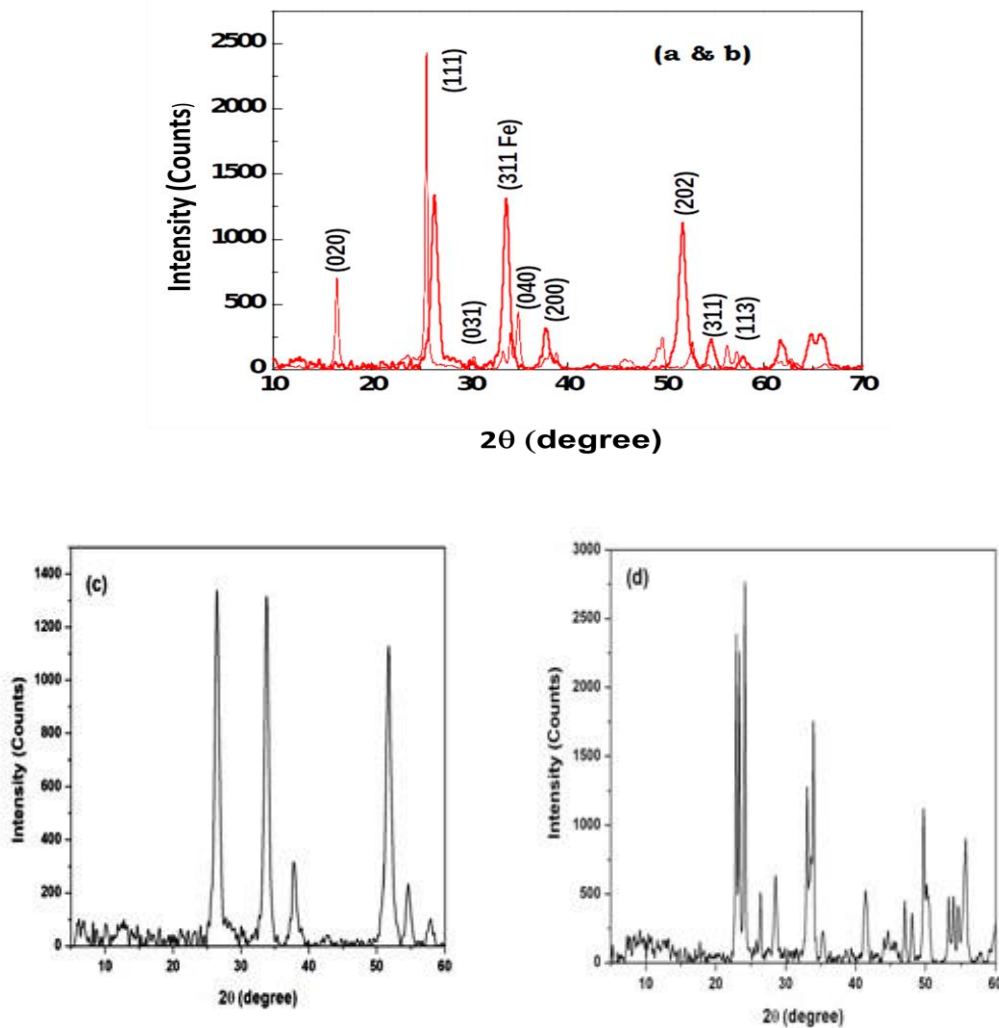


Fig.2: Powder X-ray diffraction pattern: a)  $\text{WO}_3 \cdot \text{H}_2\text{O}$  (Without doping); b)  $\text{W}_{17}\text{O}_{47}$  (Without doping); c)  $\text{WO}_3 \cdot \text{H}_2\text{O}$  (With doping); d)  $\text{WO}_3$  (With doping)

### 3.2. UV - VIS - DRS Analysis

In order to evidence the incorporation of  $\text{Fe}^{2+}$  ion in the host framework of tungsten oxide ( $\text{WO}_3$ ), the Diffusion Reflectance spectra obtained at room temperature is shown in Fig.

(3(a) to 3(d)). A clear red shift was observed for both as prepared and annealed samples since the absorption edge shifts towards higher wavelength region. The band gap energy values

of the respective prepared samples can be calculated using Kubelka – Munk function which is expressed below.

$$F(R) = \frac{(1 - R)^2}{2R}$$

Where R is the reflectance coefficient and a graph is plotted between F(R) Vs λ. The linear extrapolation of this graph will be used to calculate the band gap energy values of the respective prepared nano dimensional materials which is illustrated by the inset of Figs.(3a to 3d). The calculated values of the band gap energies were found to be 2.47 eV [23] and 3.40 eV for the samples pure and “Fe” doped WO<sub>3</sub>.H<sub>2</sub>O respectively. On the other hand the energy values of the annealed samples for both pure and doped samples to be 1.96 eV [24]

and 2.22 eV respectively. The decrease in band gap energy may be attributed due to the incorporation of Fe<sup>2+</sup> at the lattice site of W<sup>6+</sup> since both of ions having almost the same ionic radii (~ 74 – 75 pm). Also the possible reasons for narrowing the band gap both in as prepared and annealed samples should account firstly, the reduction of oxygen vacancies since the change in band gap energy is due to the difference between charge and host ions [25]. Secondly, the reduction of oxygen vacancy concentration may be attributed to the synergic effect between the donar W<sup>6+</sup> and the acceptor Fe<sup>2+</sup> ions [26] as illustrated below which are in agreement with the Powder XRD results. Therefore, It may noted that the reduction of oxygen deficiencies within the frame work of WO<sub>3</sub> were responsible for the increase in the band gap value.

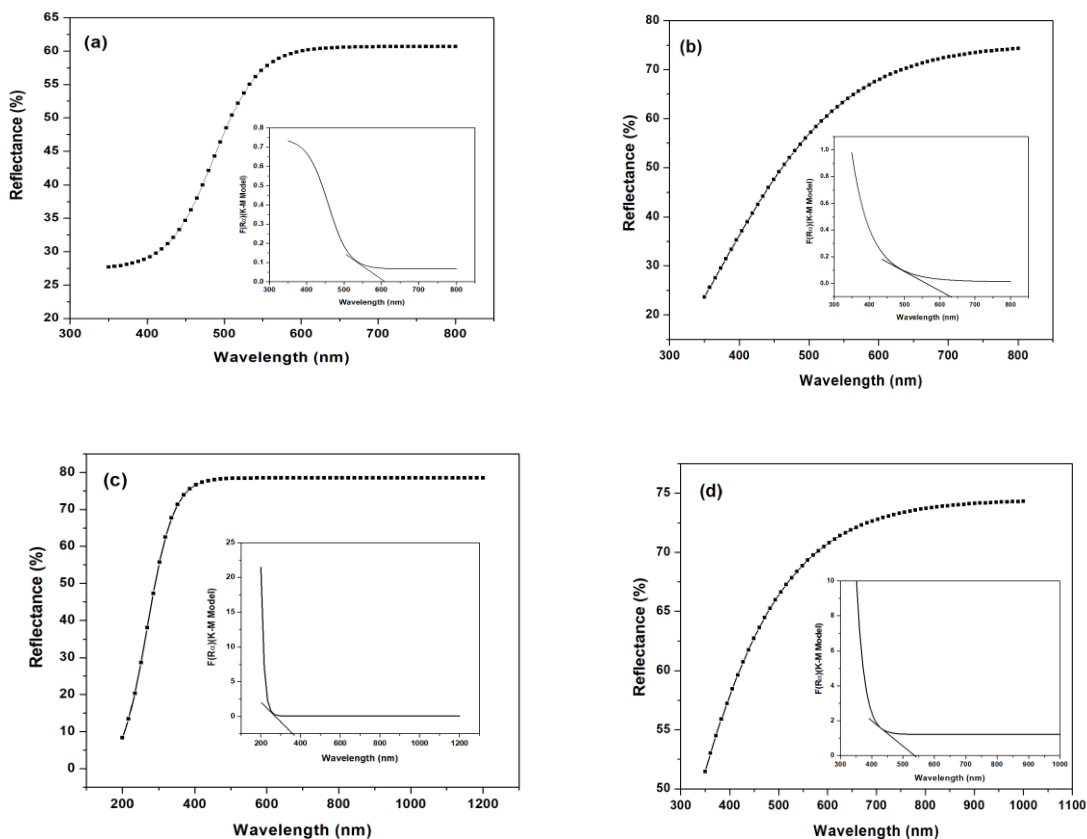
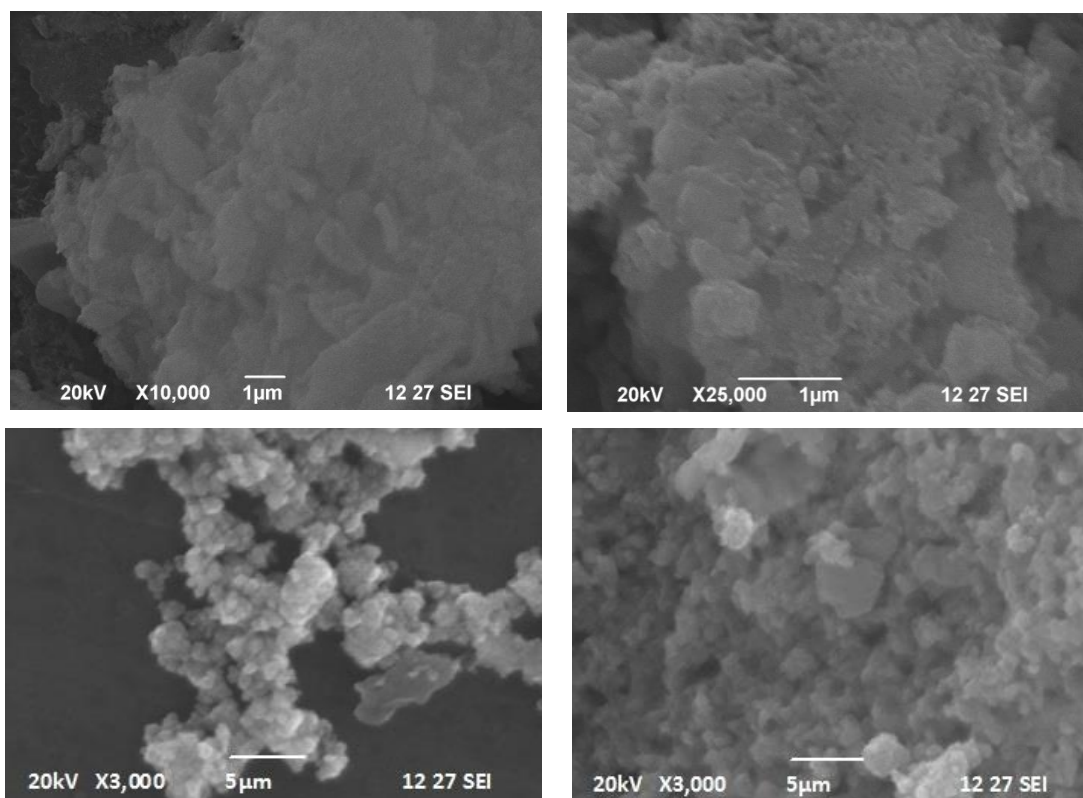


Fig.3: UV – DRS nature of: a) WO<sub>3</sub>.H<sub>2</sub>O (Without doping); b) W17O47 (Without doping); c) WO<sub>3</sub>.H<sub>2</sub>O (With doping); d) WO<sub>3</sub> (With doping)

### 3.3 Microscopic Analysis

Fig.4a-4d presents the microstructural nature of the pure and doped as prepared and annealed samples respectively. It can be seen that all the samples shows the densely occupied spherical like structure which clearly shows the anisotropic nature of the grown polycrystalline materials. Also it clearly exhibits the role of dopants in fixing the grain size of the end products. Fig. 4(a) & 4(b) indicates the scanning electron microscopic image of pure and doped

as prepared samples. As the introduction of dopant, the smaller size in grain due to the fact that the reduction of growth rate during synthesis process which is in agreement with the powder XRD results. The image shows the resultant as prepared products have a wide range of size distribution from 0.2 – 3.2  $\mu\text{m}$ . On the other hand, in the case of annealed samples (Fig. 4c & 4d) the size distribution varying from 2 – 4  $\mu\text{m}$  which indicates the size of the grains have been affected by the dopant due to growth of long crystallographic facets.



**Fig.4: FE - SEM images of: a)  $\text{WO}_3 \cdot \text{H}_2\text{O}$  (Without doping); b)  $\text{WO}_3 \cdot \text{H}_2\text{O}$  (With doping) c)  $\text{W17O47}$  (Without doping); d)  $\text{WO}_3$  (With doping)**

### 3.4 Photocatalytic Activity

Photocatalytic activity of annealed pure and “Fe” doped tungsten oxide ( $\text{WO}_3$ ) were investigated via the photo degradation of Rhodamine B dye under the illumination of UV light at room temperature. The sample of around 50mg annealed samples as catalyst were dispersed in the ratio (2:1) 80 mL / 4  $\text{mg} \cdot \text{L}^{-1}$  Rhodamine B dye with aqueous solution taken in 100mL beaker and the suspension was stirred for 45min to reach adsorption equilibrium in darkness condition. The suspension was further irradiated with 6W UV-lamp (Philips, Poland) in 254nm during continuous stirring process. 7cm distance was

maintained between the suspension and lamp. For the every 30min the sample suspension was taken, centrifuged for 5min and the concentration of rhodamine B in the suspension was finding using UV-Vis (Ocean Optics, USA) spectrophotometer. The maximum absorption of rhodamine B was found to be 553nm.

The absorption spectra for tested compounds and their degradation rate are displayed in Figures: 5 and 6(a) respectively. The linear degradation behavior of the sample clearly shows that dye is degrading under visible region (553nm) since the color of the

rhodamine B are purple in color. Degradation efficiency of the tested compounds was calculated using the below formula,

$$\text{Degradation efficiency}(\%) = \frac{A_0 - A_t}{A_0} \times 100$$

Where  $A_0$  and  $A_t$  are the absorbance at  $t = 0$  and corresponding time respectively. The obtained degradation efficiency results (Figure 6(b)) implies "Fe" doped annealed  $\text{WO}_3$  sample is having highest degradation efficiency around 46.9% due to the formation of hydroxyl radical ( $\text{OH}^\circ$ ) and super oxide radical ( $\text{O}_2^\circ$ ) at the band

gap energy value of 2.2 eV. This result is in agreement with the UV-Vis diffused reflectance spectra analysis since it retains its stoichiometric oxygen content. The photo degradation efficiency is having the following order:  $\text{WO}_3 \cdot \text{H}_2\text{O} < \text{W}_{17}\text{O}_{47} < \text{WO}_3 \cdot \text{H}_2\text{O}$  (Fe doped)  $< \text{WO}_3$  (Fe doped). The "Fe" doped  $\text{WO}_3$  nanoparticles exhibits two fold times higher efficiencies than that of the pristine samples. The structural stability was confirmed through powder XRD analysis after degradation experiments that clearly explored there is no observable change in XRD pattern. It reveals the structural stability of the tested compounds after degradation experiment.

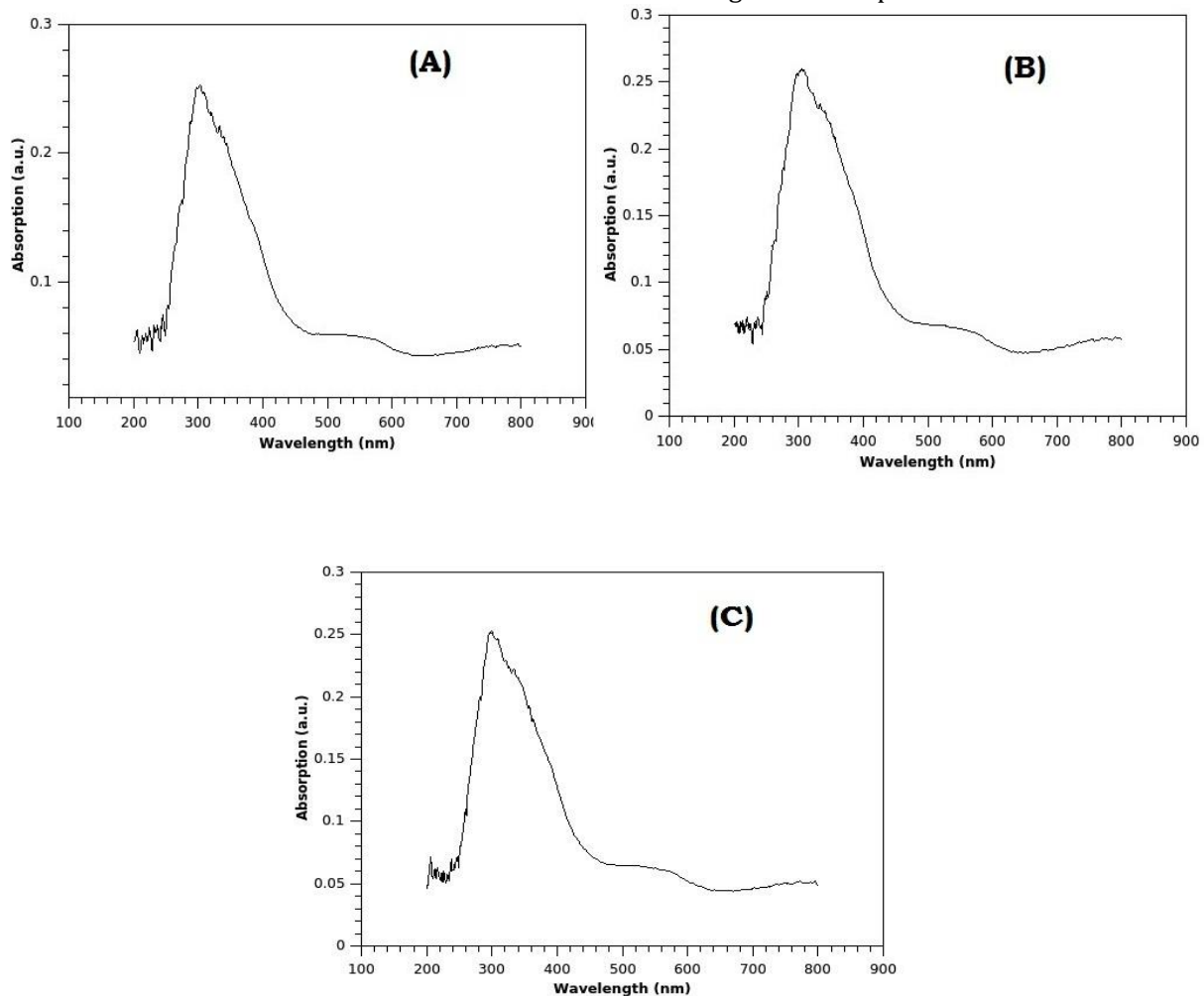


Figure5: UV-Vis absorbance spectra (a) as prepared  $\text{WO}_3 \cdot \text{H}_2\text{O}$ , (b) annealed  $\text{W}_{17}\text{O}_{47}$ , (c) annealed prepared  $\text{WO}_3 \cdot \text{H}_2\text{O}$  (Fe)

## CONCLUSION

The present work deals the polycrystalline pure and doped tungsten oxide ( $\text{WO}_3$ ) nanomaterials were prepared using facile microwave irradiation technique without employing hydrothermal method. The prepared

compounds were characterized in order to know the suitability for antibacterial activity. The powder X-ray diffraction results confirmed the phase formation and the crystalline nature of the prepared products with orthorhombic and monoclinic phase formations for the pure

Hariharan et al.,

( $\text{WO}_3 \cdot \text{H}_2\text{O}$ ) and annealed samples ( $\text{W}_{17}\text{O}_{47}$  &  $\text{WO}_3$ ) respectively. Moreover, optical behavior of the samples from UV-VIS diffusion reflectance analysis revealed that  $\text{W}_{17}\text{O}_{47}$  having remarkable band gap values due to the transfer of oxygen ions in the regions of oxygen vacancies inside the crystalline domain. The microscopic behavior of the prepared compounds were analyzed by FE - SEM and the average dimension of the prepared samples

were found to be 0.2 – 3.2  $\mu\text{m}$  and 2 – 4  $\mu\text{m}$  for the pure and annealed products respectively. The photocatalytic degradation behavior for Rhodamine B revealed that “Fe” doped  $\text{WO}_3$  nanoparticles showed high degradation efficiency of 46.9%. This result implied “Fe” doped  $\text{WO}_3$  nanoparticles may be promising candidate for dye degradation and may be applied for waste water treatment applications.

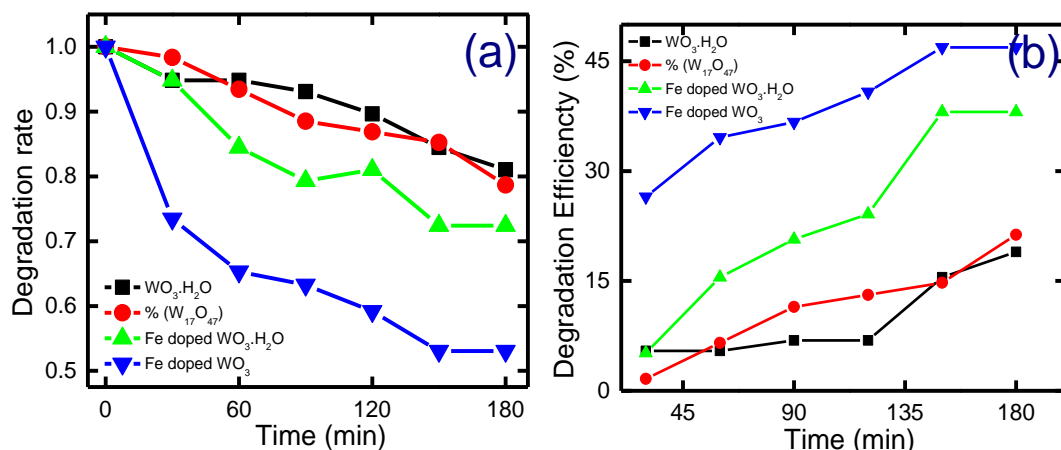


Figure6: (a) Degradation rate (b) degradation efficiency of the tested compounds

#### ACKNOWLEDGEMENT

One of the authors (VA) would like to thank DST-FIST-137/2013, Government of India for providing financial support to carry out this work

#### REFERENCES

- [1] Lassner, E., Schubert, W.D. Tungsten – Properties Chemistry Technology of the Element Alloys and Chemical Compounds, first ed., Springer, New York, (1999).
- [2] Cox, P.A. Transition Metal Oxides, Clarendon Press, Oxford, (1995).
- [3] Guangxin Duan., Lu Chen., Zhifeng Jing., Phil De Luna., Ling Wen., Leili Zhang., Lin Zhao., Jiaying Xu., Zhen Li., Zaixing Yang., Ruhong Zhou. 2019. Robust Antibacterial Activity of Tungsten Oxide ( $\text{WO}_{3-x}$ ) Nanodots. Chem. Res. Toxicol. 32, 7, 1357–1366
- [4] Hameed, A., Gondal, M.A., Yamani, Z.H. 2004. Effect of transition metal doping on photocatalytic activity of  $\text{WO}_3$  for water splitting under laser illumination: role of 3d-orbitals, Catalysis Communications, 5(11) 715-719
- [5] Umair Baig., Gondal, M. A. Suriya Rehman., Sultan Akhtar. 2020. Facile synthesis, characterization of nano-tungsten trioxide decorated with silver nanoparticles and their antibacterial activity against water-borne gram-negative pathogens, Applied Nanoscience, 10, 851–860
- [6] Rupy Kaur Matharu., Lena Ciric., Guogang Ren., Mohan Edirisinghe. 2020. Comparative Study of the Antimicrobial Effects of Tungsten Nanoparticles and Tungsten Nanocomposite Fibres on Hospital Acquired Bacterial and Viral Pathogens, Nanomaterials, 26, 1017.
- [7] Jeevitha, G., Abhinayaa, R., Mangalaraj, D., Ponpandian, N. 2018. Tungsten oxide-graphene oxide ( $\text{WO}_3$ -GO) nanocomposite as an efficient photocatalyst, antibacterial and anticancer agent, Journal of Physics and Chemistry of Solids, 116, May, 137-147
- [8] Han, B., Popov, A. L., Shekunova, T. O., Kozlov, D. A., Ivanova, O. S., Rummyantsev, A. A., Shcherbakov, A. B., Popova, N. R., Baranchikov, A. E., Ivanov V. K. 2019. Highly Crystalline  $\text{WO}_3$  Nanoparticles Are Nontoxic to Stem

- [9] Cells and Cancer Cells, Journal of Nanomaterials, Article ID 5384132  
Maqusood Ahamed., Hisham A. Alhadlaq, Majeed Khan, M. A., Ponmurugan Karuppiyah., Naif A. Al-Dhabi.2014. Synthesis, Characterization, and Antimicrobial Activity of Copper Oxide Nanoparticles, Journal of Nanomaterials, Article ID 637858
- [10] Fariba Ghasempour ., Rouhollah Azimirad ., AbbasAmini ., OmidAkhavan .2015.Visible light photo inactivation of bacteria by tungsten oxide nanostructures formed on a tungsten foil, Applied Surface Science, 338, 30 May, 55-60.
- [11] Bankier, C., Matharu, R. K., Cheong, Y. K., Ren, G. G., Cloutman-Green E., Ciric L. 2019. Synergistic Antibacterial Effects of Metallic Nanoparticle Combinations, Scientific Report, 9, Article number: 16074.
- [12] Muhammad Ali Syed, Umair Manzoor, Ismat Shah, S. Habib Ali Bukhari.2010. Antibacterial effects of Tungsten nanoparticles on the Escherichia coli strains isolated from catheterized urinary tract infection (UTI) cases and Staphylococcus aureus, New Microbiologica, 33, 329-335.
- [13] Raid A.Ismail., Ghassan M.Sulaiman., Safa A.Abdulrahman ., Thorria R.Marzoog. 2015. Antibacterial activity of magnetic iron oxide nanoparticles synthesized by laser ablation in liquid, Materials Science and Engineering: C, 53, 1 August 2015, 286-297
- [14] Hasan Türkez, Erdal Sonmez, Ozlem Turkez, Mokhtar Ibrahim Yousef, Antonio Di Stefano, Güven Turgut.2014.The Risk Evaluation of Tungsten Oxide Nanoparticles in Cultured Rat Liver Cells for Its Safe Applications in Nanotechnology, Brazilian Archives of Biology and Technology 57(4):532-541
- [15] Popov, A. L., Savintseva, I. V., Popova, N. R., Shekunova, T. O., Ivanova, O. S., Shcherbakov, A. B., Kozlov, D. A., Ivanov V. K. 2019.PVP-stabilized tungsten oxide nanoparticles (WO<sub>3</sub>) nanoparticles cause hemolysis of human erythrocytes in a dose-dependent manner, Nanosystems: Physics, Chemistry, Mathematics, 10 (2), P. 199–205
- [16] Giray Bugra Akbaba, Hasan Turkez, Erdal Sonmez, Ugur Akbaba, Elanur Aydın, Abdulgani Tatar, Guven Turgut, Salim Cerig. 2016. In vitro genotoxicity evaluation of tungsten (VI) oxide nanopowder using human lymphocytes. Biomedical Research, 27 (1): 125-130
- [17] Hariharan, V., Parthibavarman,M., Sekar,C., 2011.Synthesis of tungsten oxide (W18O49) nanosheets utilizing EDTA salt by microwave irradiation method, J. Alloy. Compd. 509 4788-4792.
- [18] Hariharan, V., Gnanavel, B., Aroulmoji, V., Sathiyapriya, R., Prabakaran, K., Sekar C. 2018. Simultaneous Structural and Optical Control of Tungsten Oxide(WO<sub>3</sub>) Nanoparticles through Cobalt Doping for Super Conducting Applications, Int. J. Adv. Sci. Eng. 4(4) 698-706
- [19] Jesionowski, T, 2002. Characterisation of silicas precipitated from solution of sodium metasilicate and hydrochloric acid in emulsion medium, Powder Technol., 127, 56–65
- [20] Bokuniaeva, A O., Vorokh. A S. 2019 Estimation of particle size using the Debye equation and the Scherrer formula for polyphasic TiO<sub>2</sub> powder, J. Phys.: Conf. Ser. 1410 012057
- [21] Gasidit Panomsuwan., Hathaikarn Manuspiya.2019. Correlation between size and phase structure of crystalline BaTiO<sub>3</sub> particles synthesized by sol-gel method, Mater. Res. Express 6 065062
- [22] Rafael Schmitt, Andreas Nanning, Olga Kraynis, Roman Korobko , Anatoly I. Frenkel, Igor Lubomirsky, Sossina M. Haile., Jennifer L. M. Rupp.2020. A review of defect structure and chemistry in ceria and its solid solutions, Chem. Soc. Rev., 49, 554-592
- [23] Priyadharshini,M., Rajesh,P., Syed Illiyas Syed Maqbool, Hariharan,V., Ezhil, I., Manimaran. 2021. Identifying the Suitability of Environmental Friendly Fe<sub>2</sub>O<sub>3</sub> Nanomaterials for Supercapacitor Applications, Elixir Nanotechnology 157 (2021) 55553-55557
- [24] Thirumoorthi, G., Gnanavel, B., Kalaivani, M., Abirami, R., Hariharan, V. 2021. Suitability of Iron (Fe)-Doped Tungsten Oxide (WO<sub>3</sub>) Nanomaterials for Photocatalytic and Antibacterial

- [25] Applications, International Journal of Nanoscience, 20, 5.  
Pridharshini, M., Rajesh,P., Manikandan, J., Hariharan,V., Ezhil Inban, M.2022. Analyzing the Suitability of Chromium Doped Iron Oxide Nanoparticles for Creatinine Bio Sensor Applications, Indian Journal of Pure and Applied Physics, 60,
- [26] Nagaraju,P., Paulraj,S., Hariharan, V., Allen Moses Samuel Elizabeth, Raghu Yuvaraj, Rajeswari,Y., Navaneetha,P., Jayavel, R.2022. Enhanced UV-Irradiated Photocatalytic Degradation of Malachite Green by Porous-WO<sub>3</sub> Decorated on 2D Graphene Sheet, Applied Biochemistry and Biotechnology, PMID: 35394253